P3.8 USE OF CERES PAPS OBSERVATIONS OVER THE VALENCIA ANCHOR STATION TO VALIDATE LOW SPATIAL RESOLUTION REMOTE SENSING DATA AND PRODUCTS.

A. Velázquez Blázquez[1], S. Alonso[2], C. Doménech[1], J. Gimeno[1], J. Jorge Sanchez[3], A. Labajo[2], N.G. Loeb[4,5], D. Pino[3,6], A. Rius[6], A. Sanchis[1], G. L. Smith[4,7], Z. P. Szewczyk[4,8], R. Tarruella[3], J. Torrobella[6], E. Lopez-Baeza[1]

(1) Climatology from Satellites Group, Dept. of Physics of the Earth and Thermodynamics, University of Valencia, Spain
(2) Spanish Institute for Meteorology, Spain
(3) Polytechnic University of Catalonia, Spain
(4) NASA Langley Research Centre (LaRC),VA, USA
(5) Hampton University, VA, USA
(6) Institute of Space Studies of Catalonia, Spain
(7) National Institute for Aerospace, Hampton, VA, USA
(8)Science Applications International Corporation, Hampton, VA, USA

ABSTRACT

The *Valencia Anchor Station* aims to develop validation studies of low-spatial resolution remote sensing data and products under the framework of the SCALES (*SEVIRI and GERB Cal/Val Area for Large Scale field ExperimentS*) Project.

The methodology so far developed has been achieved by using CERES (*Clouds and the Earth's Radiant Energy System*) observations taken in PAPS (*Programmable Azimuth Plane Scanning*) mode over the *Valencia Anchor Station* reference area.

The purpose of this work is to compare Top of the Atmosphere (TOA) radiances and fluxes measured by CERES to those simulated by STREAMER radiative transfer code fed with surface and atmospheric parameters specially gathered during the *Second GERB Ground Validation Campaign* at the *Valencia Anchor Station* in February 2004.

In this work, we include the selection of atmospheric profiles from on-purpose radiosonde and GPS (*Global Positioning System*) data, a realistic BRDF (*Bidirectional Reflectance Distribution Function*) estimation for the large-scale area and STREAMER radiative transfer simulations of TOA shortwave and longwave radiances and fluxes under clear sky and cloudy sky conditions. For cloudy sky simulations, CERES-MODIS SSF (*Single Scanner Footprint*) data has been used to get the required cloud parameters (Wielicki et al,1996).

The methodology here developed will be useful to validate the GERB (*Geostationary Earth Radiation Budget)* instrument on board METEOSAT-8).

Keywords: BRDF, CERES, Earth Radiation Budget, GERB, Valencia Anchor Station, Validation of low spatial resolution satellite data and products.

1. INTRODUCTION

The *Valencia Anchor Station* (VAS) is an automatic meteorological station equipped with a large number of instruments to carry out validation activities of low spatial-resolution remote sensing data and products . It is placed in a reasonably homogeneous and flat area of about 50x50 km^2, mainly dedicated to vineyards, including some other typical Mediterranean ecosystem species such as shrubs, olive and almond trees and alepo pine forests, being the latter only present in a small mountain formation in the area (Velázquez, 2004)

In order to perform those validation tasks, several validation campaigns have been carried out in the study area, measuring the surface and atmospheric parameters needed. Both Terra FM2 and Aqua FM3 CERES measurements were available for the campaigns. Usually, CERES operates in *Cross-Track* mode, that is, it looks at the surface in the orthogonal plane of its orbit, but it can also be programmed to scan over a determined area azimuthally changing the observation plane (*Programmable Azimuth Plane Scanning* Mode, PAPS), thus optimizing validation studies (Figure 1). This mode of operation provides a wide database of radiances and fluxes over the area being this the mode in which CERES Terra FM2 and Aqua FM3 worked during the *Second GERB Ground Validation Campaign* held in the *Valencia Anchor Station* area between 9th and 12th of February 2004.

In this work, we will show the comparison between CERES TOA radiances and STREAMER simulated TOA radiances. In the STREAMER radiative transfer code, radiances and fluxes are computed by using the discrete ordinate solver, DISORT version 2 (Stamnes et al, 2000).

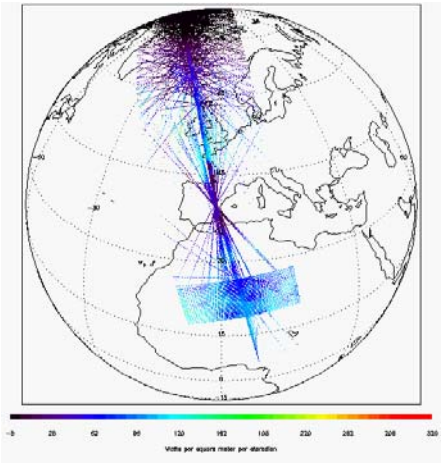

Figure 1. Sample of CERES FM3 TOA Shortwave Radiances over the VAS. 12th February 2004.

The surface and atmospheric parameters used in the simulations were gathered in the campaign and include two radiosounding ascents per day temporally close to the CERES observations, integrated water vapour from simultaneous measurements of zenith tropospheric delay from GPS, measurements of atmospheric transmissivity, and radiation measurements from the VAS and from a mobile station placed on a low-vegetation trees and shrubs area.

2. METHODOLOGY

In order to be able to reproduce CERES observations, it will be needed a good characterization of the surface and of the atmosphere. Moreover, in order to get good agreement in the shortwave range, the anisotropy of the radiation field is absolutely needed to be taken into consideration. Thus, a careful parameter selection will be crucial in validation tasks.

2.1 Selection of Atmospheric profiles

Radiosoundings ascents provide pressure, temperature and humidity profiles. The water vapour profile is obtained by scaling the total water vapour content to the integrated water vapour measured by the GPS. Thus, we take good advantage of the better temporal resolution of GPS data and also keep the profile of water vapour in the troposphere. Moreover, the correlation between both measurements is really high (figure2)

As far as the aerosol profile is concerned, we use the STREAMER MLW (*Mid-Latitude Winter*) standard atmosphere profile, assuming background tropospheric aerosols and background stratospheric aerosols, with the aerosol optical depth obtained from the on-ground transmissivity measurements.

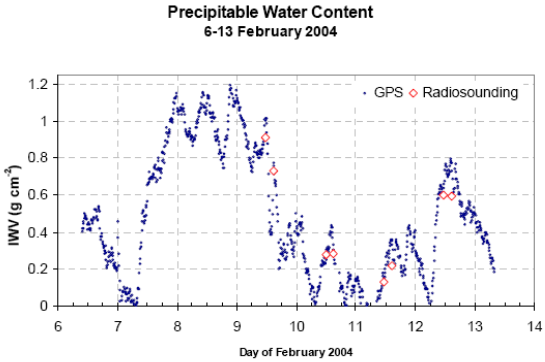

Figure 2: Comparison between precipitable water content measurements from the GPS receiver (red diamonds) and from the radiosounding ascents (blue squares)

The ozone profile corresponds to the STREAMER *Mid Latitude Winter* one scaled to the TOMS (*Total Ozone Mapping Spectrometer*) measurements. (http://toms.gsfc.nasa.gov)

2.2 Selection of surface parameters

Surface emissivity (Wilber et al, 1999) is obtained from CERES/SARB (*Surface and Atmospheric Radiation Budget)* database (http://www-surf.larc.nasa.gov/surf/).

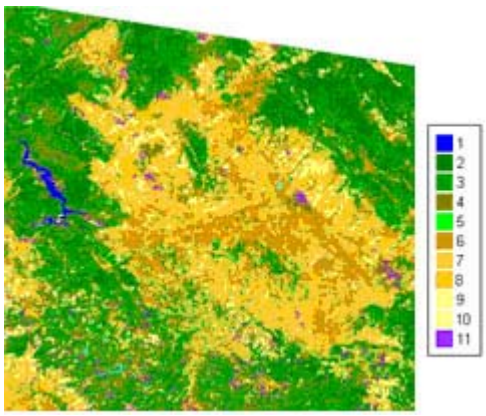

Figure 3. Land use Classification of the study area. 1.water, 2. pine trees, 3. low density pine trees and shrubs, 4. shrubs, 5. irrigated crops, 6. vineyards, 7. low density vineyards, 8. very low density vineyards, 9. herbal crops, 10. bare soil, 11. urban areas.

Surface temperatures were measured at the VAS and at the mobile station, weighting the contribution of each one in the whole area by taking into account the land use classification of the study area (Figure 3). According to that, and considering that in winter vineyards have the same behaviour as bare soil (Figure 4), we could assume that the area in winter is composed of about 33% of bare soil and 67% of vegetation (mainly shrubs and pine trees).

Figure 4. Vineyards over the study area in winter season.

In addition, it must be considered that radiances at the TOA are sensitive to the anisotropy of surface reflectance and how it varies during the day. For this reason, spectral albedo and bidirectional reflectance are key parameters to be used. We have calculated a BRDF for our study area from three contributions, namely broadband albedo weighted from those measured at the VAS and at the mobile station (α_0^{BB}), spectral albedo for the same type of soil from the *ASTER Spectral library John Hopkins University* (α_λ^{JHU}), and from bidirectional reflectance measurements ($\rho_\lambda(\theta_0, \theta, \phi)$) over bare soil from Ahmad and Deering, 1992. First, we scale spectral albedo to broadband albedo:

$$a'_\lambda = \frac{a_\lambda^{JHU}}{\int_{\lambda_1}^{\lambda_2} a_\lambda^{JHU} d\lambda} a_{BB}^0 \qquad (1)$$

Where λ_1 and λ_2 define the spectral band where the albedometers work. Then, we scale the bidirectional reflectances to the new spectral albedo value (α'_λ), being the scale factors for the bidirectional reflectances

$$s_i = \frac{a'_{\lambda_i}}{\frac{1}{\pi}\int_0^{2\pi}\int_0^1 \rho_\lambda(\theta_0,\theta,\phi)\mu \cdot d\mu \cdot d\phi} = \frac{a'_{\lambda_i}}{\rho_\lambda(\theta_0)} \qquad (2)$$

where i stands for red or NIR band and θ_0 for *Solar Zenith Angle* (SZA), θ_0 for *Viewing Zenith Angle* (VZA) and ϕ for *Relative Azimuth Angle* (RAA). The BRDF obtained for the red band is shown in Figure5.

Now we have solved the problem of choosing a BRDF directly from the bibliography, i.e, we have assumed the same anisotropy and spectral pattern but avoiding errors due to the possible consideration of a more or less bright/dark surface.

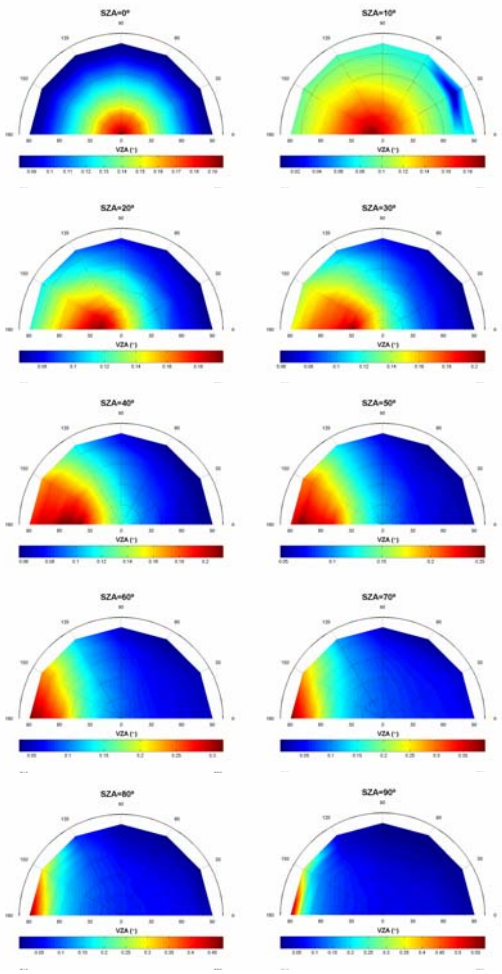

Figure. 5. Bidirectional reflectance distribution function (BRDF) at 0.662 μm. The radial axis corresponds to different VZAs, the azimuthal angle corresponds to different RAAs, and every diagram corresponds to a different SZA from 0º to 90º.

2.3 Satellite data

For CERES data, we have selected SSF products which also contains PSF (*point spread function*) CERES weighted imager parameters that will be useful to simulate cloudy sky conditions. For Terra FM2, Edition 2B data will be used and for Aqua FM3, Edition 1B.

First we check the presence of clouds over the study area. Days from 10th to 12th of February are under perfect clear sky conditions as we can infer from the cloud parameter from the SSF data and from the radiation measurements carried out at the VAS (Figure 6).

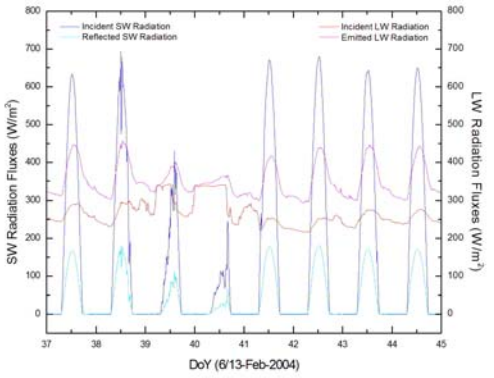

Figure 6: Shortwave and longwave surface fluxes from 6th to 13th February 2004.

9th of February is classified as a cloudy day with cloud fraction between 99% and 100% for the 77.68% of the footprints and between 40% and 99% for the rest of the data. All footprints are classified as one level, liquid water, low cloud with an effective pressure greater than 680 mb, and with optical thickness greater than 22.63. For STREAMER simulations, some SSF parameters have been selected as inputs to the model such as cloud top pressure (Figure 7), cloud optical thickness (Figure 8), cloud effective radius (Figure 9), and cloud liquid water path (Figure 10).

With all the parameters fixed, we have run two simulations per each CERES footprint, corresponding to the shortwave and longwave radiances. We keep the same observation geometry than CERES, i.e, same SZA, VZA, and RAA configuration and for cloudy conditions, we also introduce cloud top pressure, visible optical depth, effective radius and liquid water path for each footprint

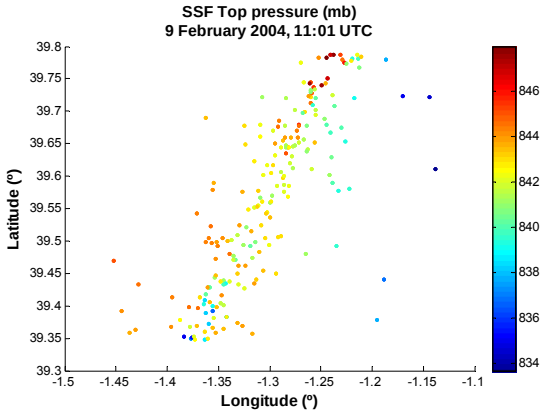

Figure 7. SSF-93, mean cloud top pressure (mb) for cloud layer in the 50x50km² area.

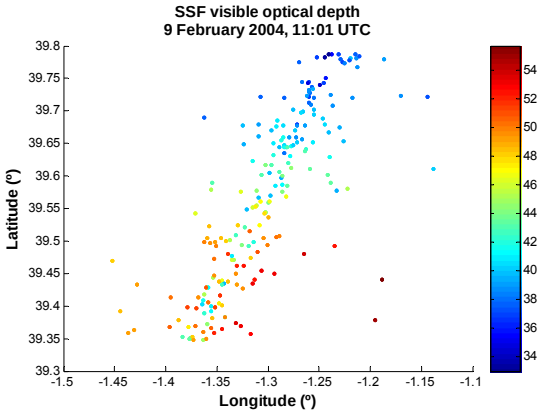

Figure 8. SSF-83, mean visible optical depth for cloud layer in the 50x50km² area.

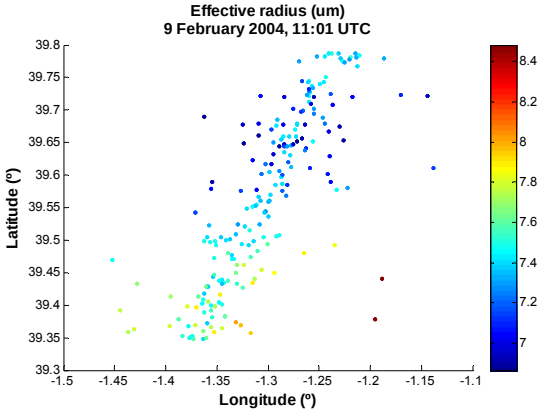

Figure 9. SSF-103, mean water particle radius for cloud layer (μm) for cloud layer in the 50x50km² area.

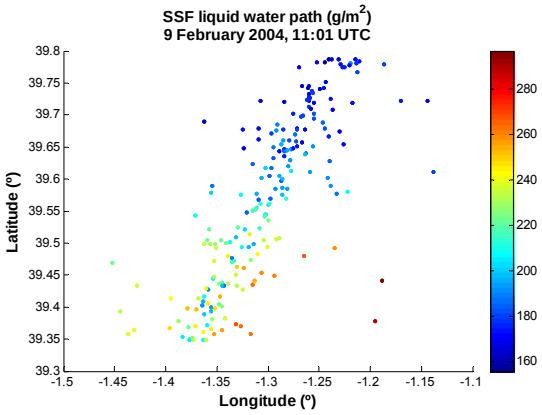

Figure 10. SSF-89, mean liquid water path (g/m²) for cloud layer in the 50x50km² area.

.

3. RESULTS

3.1 TOA Radiance comparisons

The results of the radiance simulations performed are shown in firgures with odd number from 11 to 25. From the pictures, it is easy to see the radiance

anisotropy between the *forward* and *backward* scattering directions.

In the 9th of February, we can see that the stratus cloud has high albedo, so that the amount of solar energy reflected at the TOA is high. These clouds significantly reduce the amount of solar energy absorbed by the Earth system. Figure 12 shows the SW radiances in a polar plot to illustrate that the forward scattering radiances are much higher than the backward ones under cloud sky conditions.

Figure 11, shows the preliminary results of the comparison between CERES TOA SW radiances and simulations. The modeled radiances are always overestimated in the forward scattering direction, being these differences greater as the VZA increases. Nevertheless, there is a really good agreement between CERES TOA LW radiances and STREAMER simulations.

Differences between simulated and measured shortwave radiances may be due to small changes in droplet size that could induce large changes in cloud albedo. It has been estimated, for example, that the reduction of the effective diameter of stratus cloud droplet sizes from 20 to 16 μm would balance the warming due to doubling atmospheric CO_2 (Slingo 1990). Therefore, accurate determination of the microphysical properties of boundary layer stratus is essential for the correct treatment of these clouds in radiative transfer and global climate models. (N.L. Miles, 1999)

Under clear sky conditions, the agreement is very good between satellite data and simulations, showing low RMSE (Table 1), and in all the cases analysed, it is seen that the backward radiances are always higher than the forward ones, both in the short wave and less pronounced in the longwave. This anisotropy varies with the RAA, with a minimum in the ortogonal plane (plane where observation and ilumination planes are orthogonal) and with a maximum in the principal plane (when those planes are colinear). The anisotropy on clear scenes depends on SZA, specially in the shortwave, being the longwave dependence possibly due to changes in boundary layer temperatures during the day (Minnis et al, 2004).

3.2 TOA Flux comparisons

TOA Flux comparisons have been made at a reference level of 20 km. This effective TOA has been determined as the optimal reference level for defining TOA fluxes in Earth Radiation Budget studies. This definition simplifies comparisons with plane-parallel modeled fluxes, since, at this level, there is no need to consider horizontal transmission of solar radiation through the atmosphere. (Loeb et al, 2002)

Results of these comparisons for clear sky are preliminary and are shown in figures 27 to 40. The plots show SSF CERES TOA Flux, mean of SSF CERES TOA Flux over the 50x50 km^2 and the result of STREAMER simulated Flux for the whole area. SSF TOA Fluxes have been classified regarding to the scattering direction they come from, using blue dots for fluxes derived from forward scattered radiances and green dots for fluxes derived backward scattered radiances.

The variation in CERES fluxes observed when VZA increases may be explained as a higher contribution of vegetation areas to the flux, since field of view increases as VZA does. (Figure 3).

Differences found between simulated and measured fluxes are due to the fact that there is only one STREAMER flux simulation for the whole area, without taking into account surface albedo changes in the area and, therefore, the different fluxes corresponding to each footprint. To overcome this and as a continuation of this work, surface reflectances from MOD43 product (*Surface Reflectance BRDF/Albedo Parameter*) will be considered to compute a TOA flux for every single footprint. Hence, the method will definitely improve the comparisons of fluxes derived form surface parameters to those estimated from CERES TOA observations.

Under overcast conditions (9th February), we have simulated a flux for each CERES footprint by using the same cloud parameters as for the radiance simulations. Figure 41 shows that STREAMER simulated shortwave fluxes are overestimated with respect to the CERES ones, as it was expected from the behaviour of the simulated

TIME OF CERES PAPS SCAN	RMSE FOR SW RADIANCES ($W\ M^{-2}\ SR^{-1}$)	RMSE FOR LW RADIANCES ($W\ M^{-2}\ SR^{-1}$)
9th of Feb at 11:01 UTC	25.1	3.2
10th of Feb at 13:20 UTC	7.6	1.3
10th of Feb at 11:44 UTC	4.9	3.7
11th of Feb at 10:50 UTC	6.2	2.0
11th of Feb at 12:26 UTC	3.9	1.3
11th of Feb at 14:04 UTC	8.1	1.4
12th of Feb at 11:32 UTC	4.7	1.4
12th of Feb at 13:08 UTC	4.4	2.1

Table 1: RMSE ($W\ m^{-2}\ sr^{-1}$)

radiances. As regards longwave fluxes the agreement is good.

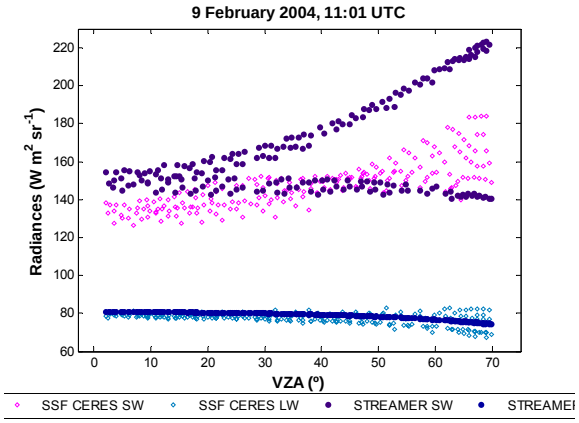

Figure 11: TOA radiances comparison for Terra FM2, 9th February 2004

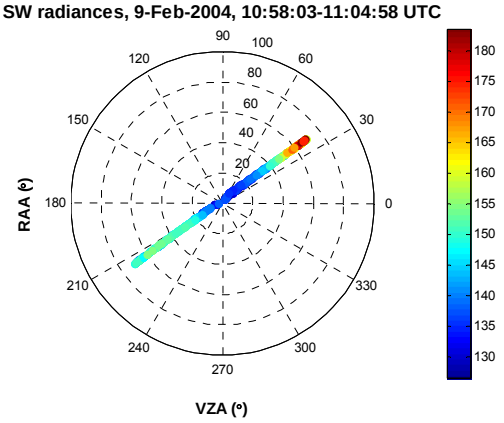

Figure 12: CERES TOA SW radiances and geometry. Radial axis corresponds to VZA and azimuthal direction corresponds to RAA.

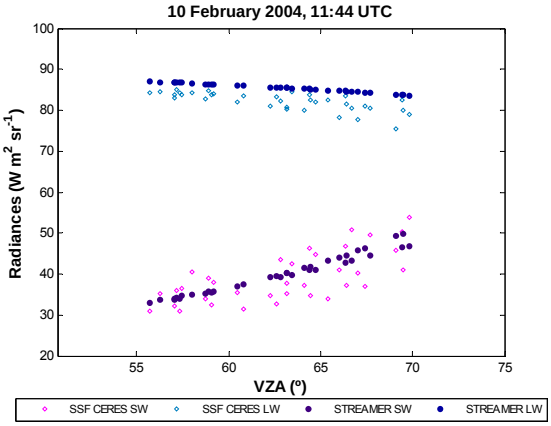

Figure 13: TOA radiances comparison for Terra FM2, 10th February 2004

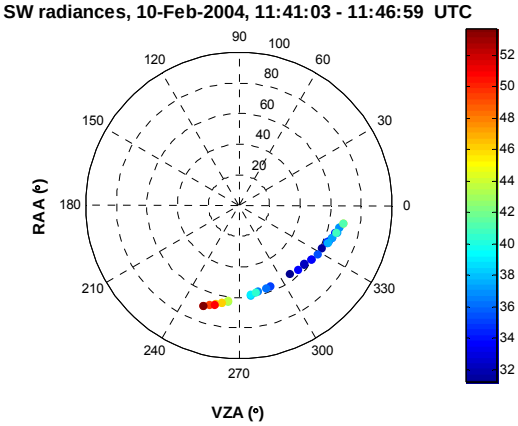

Figure 14: CERES TOA SW radiances and geometry. Radial axis corresponds to VZA and azimuthal direction corresponds to RAA.

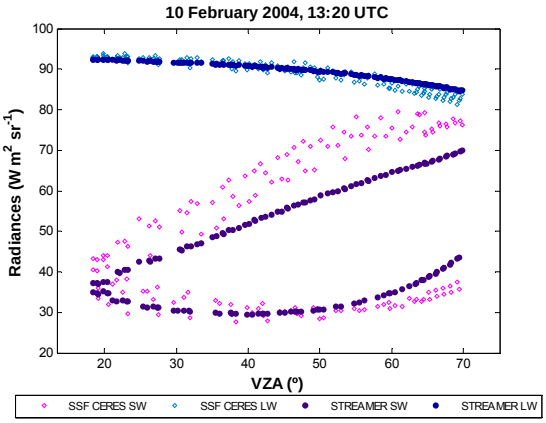

Figure 15: TOA radiances comparison for Aqua FM3, 10th February 2004

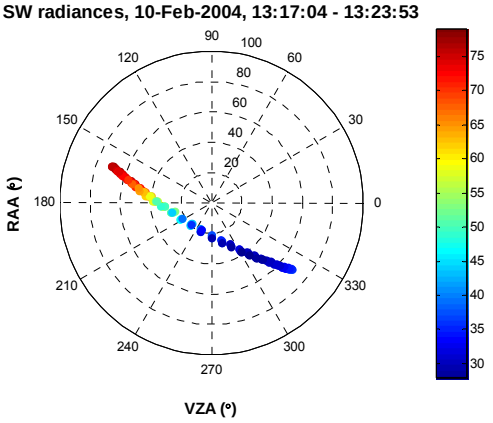

Figure 16: CERES TOA SW radiances and geometry. Radial axis corresponds to VZA and azimuthal direction corresponds to RAA.

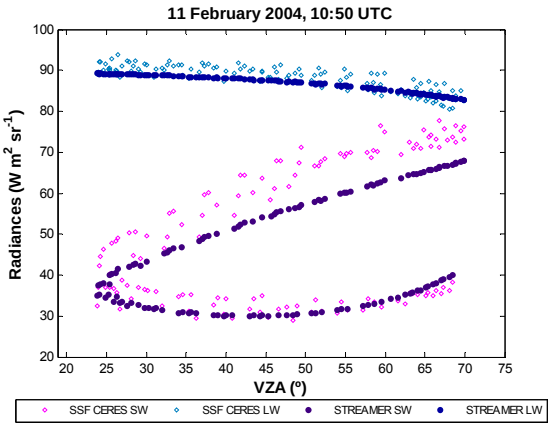

Figure 17: TOA radiances comparison for Terra FM2, 11th February 2004

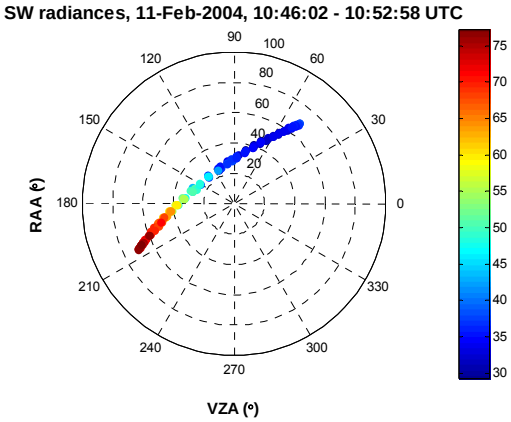

Figure 18: CERES TOA SW radiances and geometry. Radial axis corresponds to VZA and azimuthal direction corresponds to RAA.

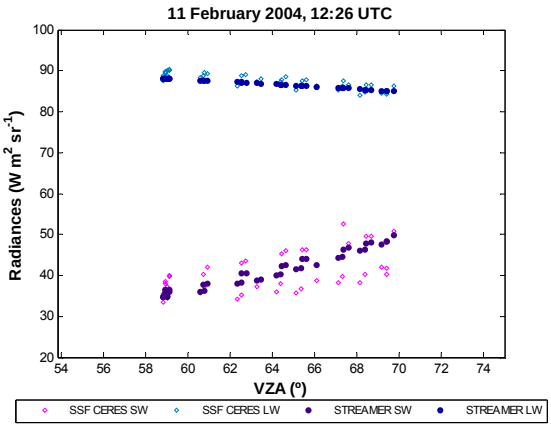

Figure 19: TOA radiances comparison for Aqua FM3, 11th February 2004

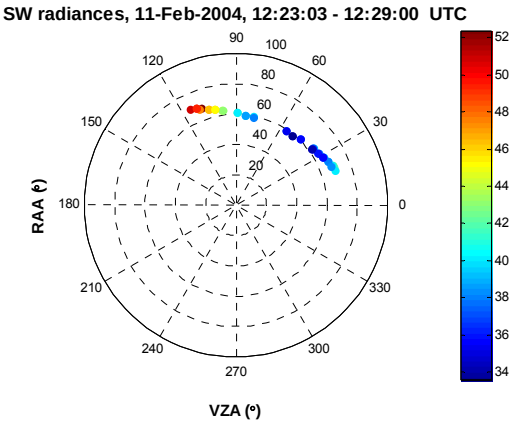

Figure 20: CERES TOA SW radiances and geometry. Radial axis corresponds to VZA and azimuthal direction corresponds to RAA.

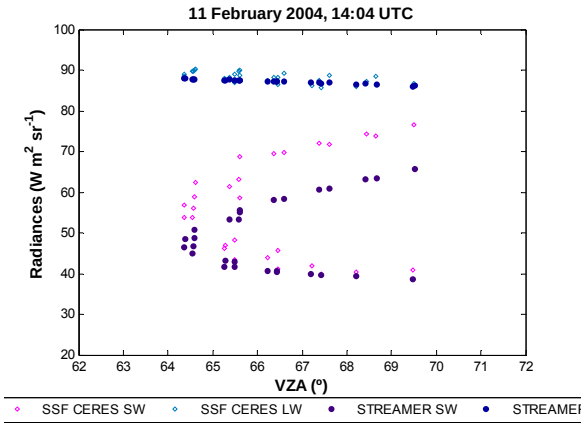

Figure 21: TOA radiances comparison for Aqua FM3, 11th February 2004

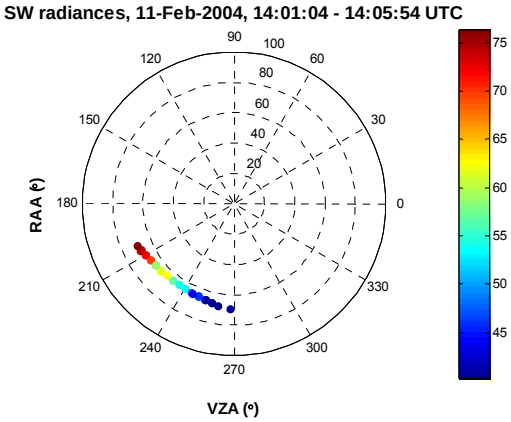

Figure 22: CERES TOA SW radiances and geometry. Radial axis corresponds to VZA and azimuthal direction corresponds to RAA.

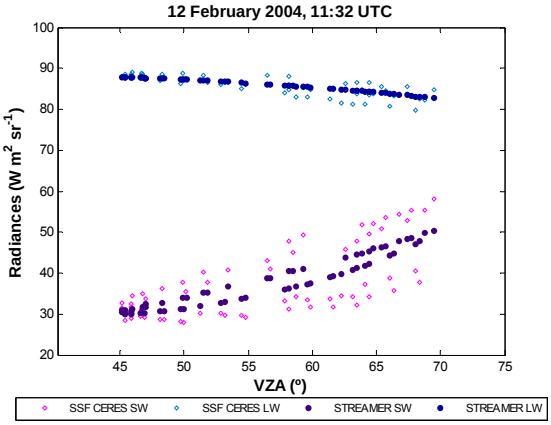

Figure 23: TOA radiances comparison for Terra FM2, 10th February 2004

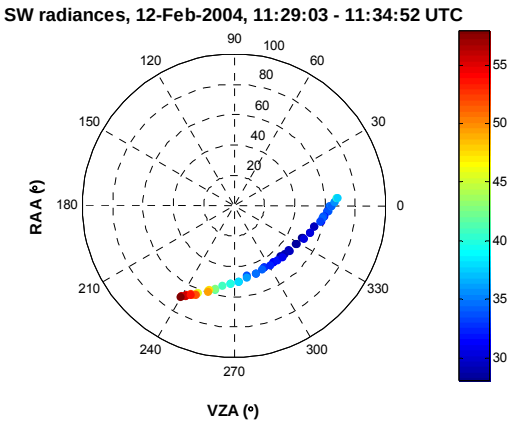

Figure 24: CERES TOA SW radiances and geometry. Radial axis corresponds to VZA and azimuthal direction corresponds to RAA.

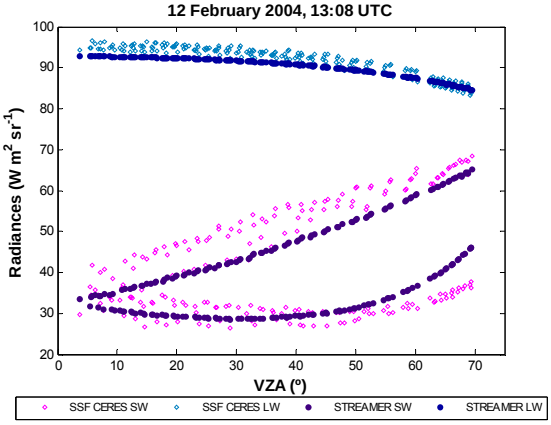

Figure 25: TOA radiances comparison for Aqua FM3, 12th February 2004

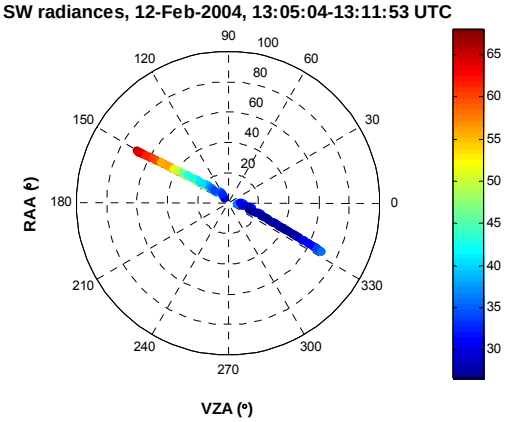

Figure 26: CERES TOA SW radiances and geometry. Radial axis corresponds to VZA and azimuthal direction corresponds to RAA.

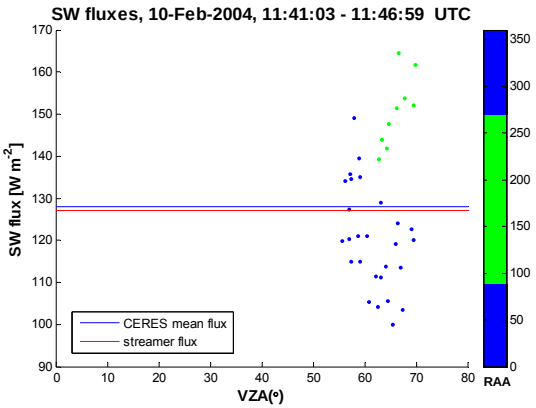

Figure 27: SW TOA Fluxes Comparison for Terra FM2, 10th February 2004

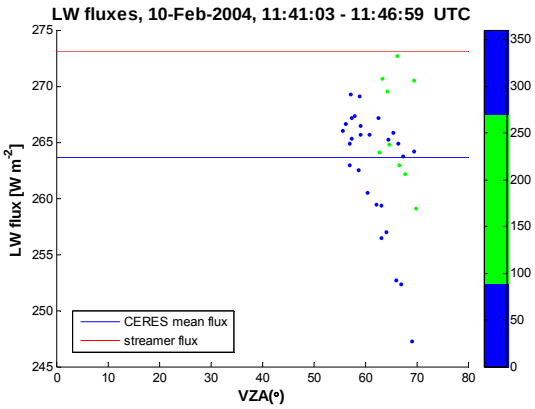

Figure 28: LW TOA Fluxes Comparison for Terra FM2, 10th February 2004

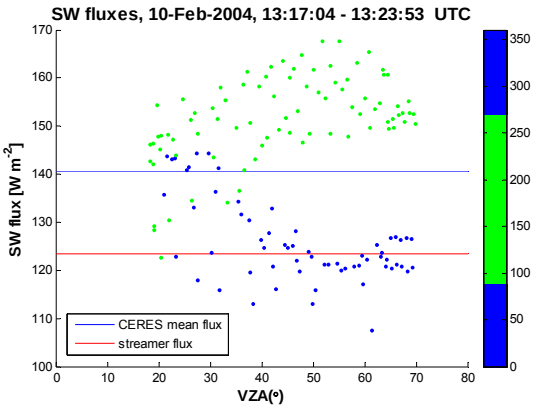

Figure 29: SW TOA Fluxes Comparison for Terra FM2, 10th February 2004

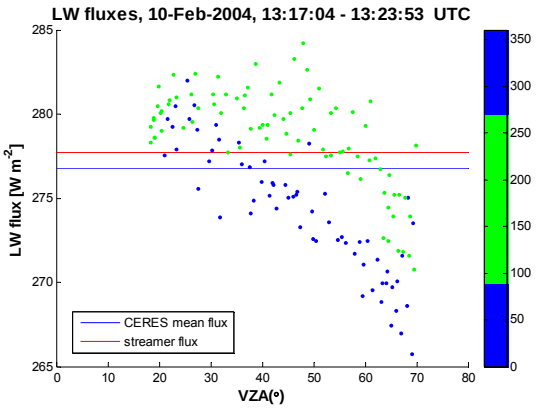

Figure 30: LW TOA Fluxes Comparison for Terra FM2, 10th February 2004.

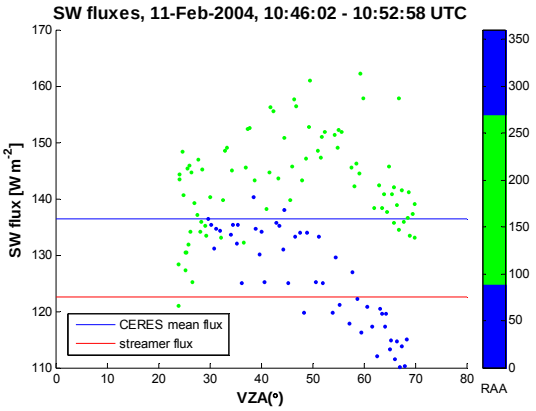

Figure 31: SW TOA Fluxes Comparison for Terra FM2, 11th February 2004

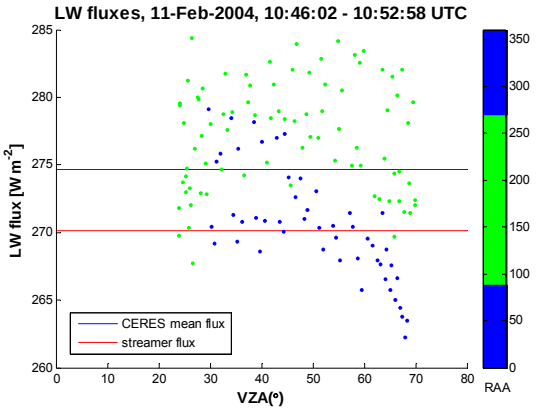

Figure 32: LW TOA Fluxes Comparison for Terra FM2, 11th February 2004.

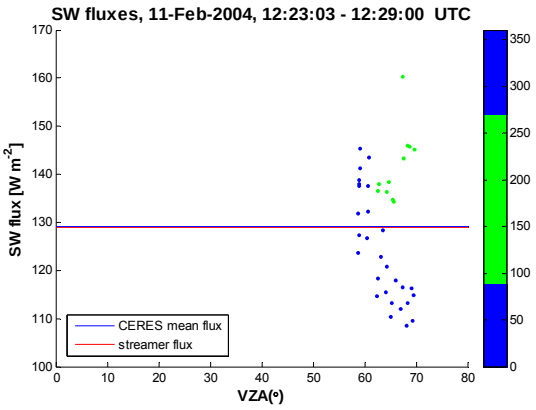

Figure 33: SW TOA Fluxes Comparison for Terra FM2, 11th February 2004

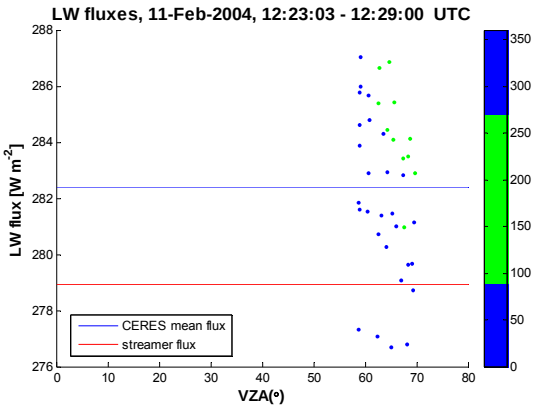

Figure 34: LW TOA Fluxes Comparison for Terra FM2, 11th February 2004.

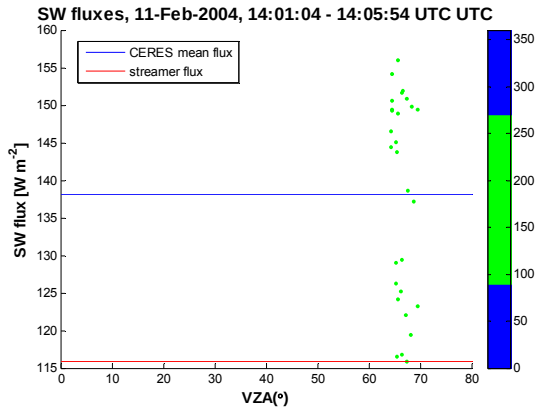

Figure 35: SW TOA Fluxes Comparison for Terra FM2, 11th February 2004

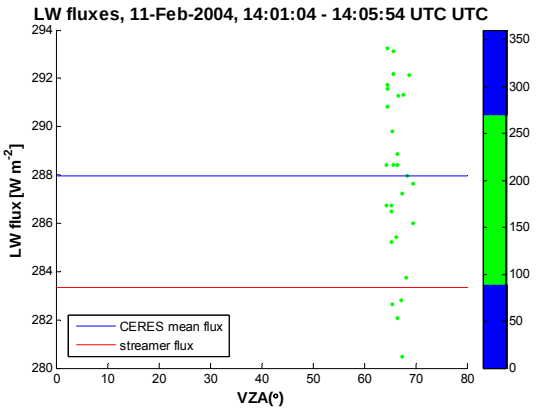

Figure36: LW TOA Fluxes Comparison for Terra FM2, 11th February 2004.

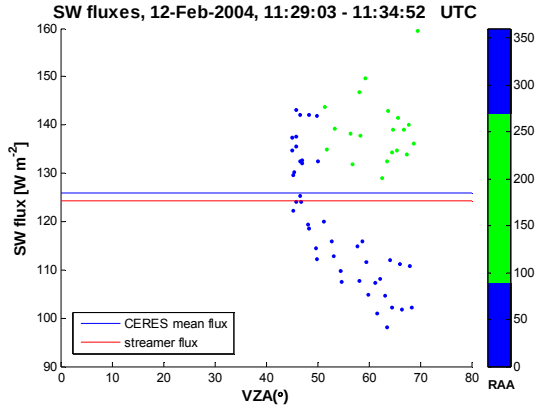

Figure 37: SW TOA Fluxes Comparison for Terra FM2, 12th February 20042

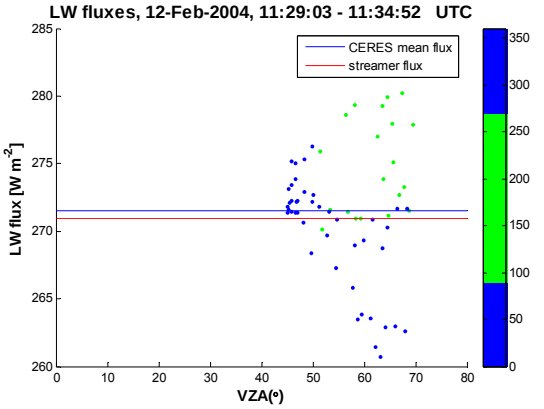

Figure 38: LW TOA Fluxes Comparison for Terra FM2, 12th February 2004.

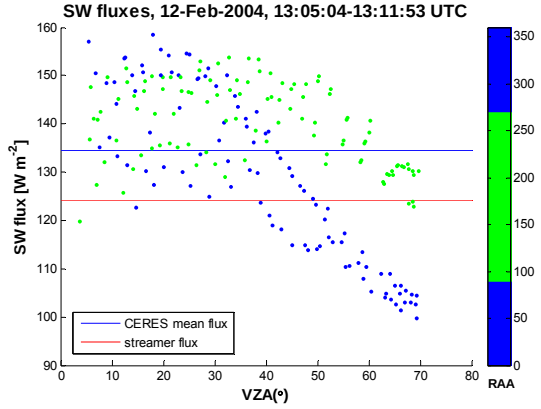

Figure 39: SW TOA Fluxes Comparison for Terra FM2, 12th February 2

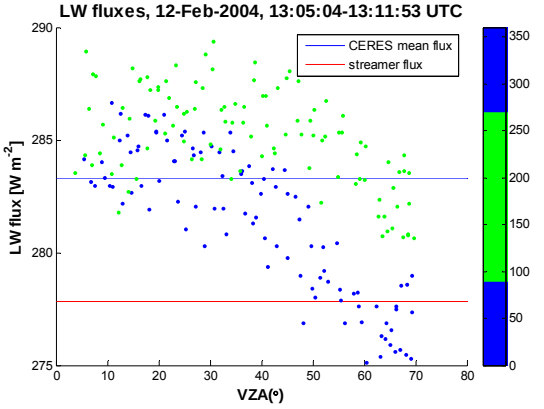

Figure 40: LW TOA Fluxes Comparison for Terra FM2, 12th February 2004.

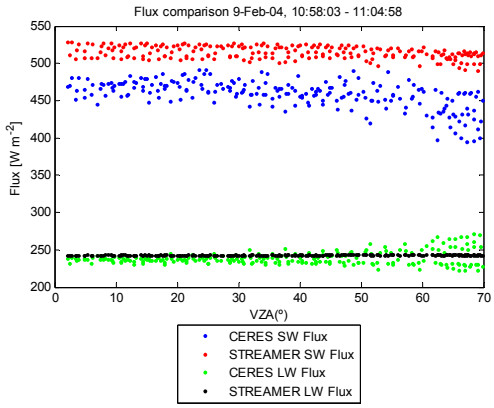

Figure 41: TOA Fluxes Comparison for Terra FM2, 9th February 2004.

4. CONCLUSIONS

We have carried out two radiance simulations for each CERES footprint, one for shortwave and the other for longwave. The number of footprints for each CERES PAPS over the 50x50 km^2 area are shown in Table 2.

Time of CERES PAPS scan	Number of footprints
9th of Feb at 11:01	215
10th of Feb at 13:20	146
10th of Feb at 11:44	36
11th of Feb at 10:50	131
11th of Feb at 12:26	39
11th of Feb at 14:04	28
12th of Feb at 11:32	63
12th of Feb at 13:08	206

Table 2. Number of footprints per CERES PAPS observation

The methodology here developed is able to reproduce CERES TOA unfiltered radiances under clear sky conditions. Simulated radiances reproduce accurately the anisotropy of the radiance field. RMSEs for clear sky conditions are lower than 8 W $m^{-2}sr^{-1}$ (Table 1).

The methodology to simulate fluxes both at the TOA and at the surface is still in a first stage of development. The inclusion of a higher resolution BRDF in the procedure should improve the comparison between simulated and CERES fluxes.

Shortwave radiances from overcast conditions are difficult to be simulated. However, LW radiances under these cloudy conditions are well reproduced.

Although the agreement between simulated and CERES longwave fluxes is good, the shortwave overestimation of the simulated radiances leads to an overestimation of the simulated fluxes as well.

CERES dedicated PAPS observations over the VAS are of great value to develop the methodology to validate low spatial resolution remote sensing data and products. In this way, the methodology is being extended and applied to GERB products.

5. REFERENCES

Ahmad, S.P. and D. W. Deering (1992): A simple Analytical Function for Bidirectional Reflectance. *J. Geophys. Res.*,**97**, D17, pages 18867-18886

Cox, C. and W.H. Munk (1954): The measurement of the roughness of the sea surface from photographs of the sun glitter. *J. Opt. Soc. Am.*, **44**, 838-850

Key, J. and A.J. Schweiger (1998): Tools for atmospheric radiative transfer: Streamer and FluxNet, *Computers & Geosciences*, **24**(5), 443-451.

Loeb, N. G., N. Manalo-Smith, S. Kato, W. F. Miller, S. Gupta, P. Minnis, and B. A. Wielicki (2002): Angular distribution models for top-of-atmosphere radiative flux estimation from the Clouds and the Earth's Radiant Energy System instrument on the Tropical Rainfall Measuring Mission Satellite. Part I: Methodology. *J. Appl. Meteor*, **42**, pages 240-264

Loeb, N.G, S. Kato and B.A.Wielicki. Defining Top-of-Atmosphere Flux Reference Level for Earth Radiation Budget Studies. *Journal of Climate*, vol: **15**, nº22, pp3301-3309.

Lopez-Baeza, E., S. Alonso, M.J. Bates, A. Bodas, S. Dewitte, C. Diaz-Pabon, C. Domenech, J.F. Gimeno Ferrer, J.E. Harries, J. Jorge, A. Labajo, N. Pineda, D. Pino, A. Rius, F. Rocadenbosch, J.E. Russell, M. Sicard, G.L. Smith, Z. Peter Szewczyk, R. Tarruella, J. Torrobella, and A. Velazquez (2004a): First GERB/CERES Ground Validation Campaign at the Valencia Anchor Station (Spain). *The 2004 EUMETSAT Meteorological Satellite Conference*. Prague, 31 May-4 June 2004

Lopez-Baeza, E., Belda, F., Bodas, A., Crommelynck, D., Dewitte, S., Domenech, C., Gimeno, J., Harries, J., Jorge, J., Pineda, N., Pino, D., Rius, A., Saleh, K., Tarruella, R., Velazquez, A. (2003): SCALES: SEVIRI and GERB CAL/VAL area for lage-scale field experiments. *Remote Sensing of Clouds and the Atmosphere VIII. Proc. Of SPIE*. Vol **5235**, pp134-148

Lopez-Baeza, E., A. Velazquez, and the SCALES PROJECT TEAM (2004b): Towards a methodology

for the validation of low spatial resolution remote sensing data and products. The Valencia Anchor Station. Committee on Space Research (COSPAR). *35th COSPAR Scientific Assembly. Scientific Commission A: Space Studies of the Earth's Surface, Meteorology and Climate. Biological and Physical Processes on Land*. Paris, France, 18 – 25 July 2004

Miles, N.L., J. Verlinde, and E.E. Clothiaux (1999). Cloud Droplet Size Distributions in Low-Level Stratiform Clouds. *Journal of Atmospheric Sciences*, Vol **57**, 295-311.

Minnis P., A.V. Gambheer and D. R. Doelling (2004): Azimuthal anisotropy of longwave and infrared window radiances from the Clouds and Earth Radiant Energy System on the Tropical Rainfall Measuring Mission and Terra data. *J. Geophys. Res.,* **109**, D08202.

Slingo, A., 1990: Sensitivity of the Earth's radiation budget to changes in low clouds. *Nature*, **342**, 49-51.

Stamnes, K., S.C. Tsay, Wiscombe and I. Laszlo, (2000): A general-purpose, numerically stable computer code for Discrete-Ordinate-Method Radiative Transfer in Scattering and Emitting Layered Media, DISORT Report v1.1

Velázquez, A. E. Lopez-Baeza, , G.L Smith, Z. P. Szewczyk (2004). CERES Operations for the Valencia Anchor Station in Support of GERB Validation Efforts. CERES SCALES Campaigns (2004). 13th Conference on Satellite Meteorology and Oceanography. Norkfolk, Virginia 20-23 September 2004.

Velazquez, A. S. Alonso, A. Bodas-Salcedo, S. Dewitte, C. Domenech, J. Gimeno, J.E. Harries, J. Jorge Sanchez, A. Labajo, N. G. Loeb, D. Pino, A. Sanchis, G.L. Smith, Z. Peter Szewczyk, R. Tarruella, J. Torrobella, E. Lopez-Baeza (2005). Comparison of top of the atmosphere GERB measured radiances with independent radiative transfer simulations obtained at the Valencia Anchor Station area. *Remote Sensing of Clouds and the Atmosphere X. Proc of SPIE 5979*

Wielicki, B. A., B. R. Barkstrom, E. F. Harrison, R. B. Lee III, G. L. Smith, and J. E. Cooper, (1996): Clouds and the Earth's Radiant Energy System (CERES): An Earth Observing System Experiment, *Bull. Amer. Meteor. Soc*., **77**, 853-868.

Wilber, A.C., D.P. Kratz, and S.K. Gupta (1999): Surface Emissivity Maps for Use in Satellite Retrievals of Longwave Radiation. *NASA/TP-1999-209362*

6. ACKNOWLEGMENTS

This work has been carried out in the framework of the SCALES Project of the *Spanish Programme on Space Research (Ministry for Science and Education)*. One of us (A. Velazquez) holds a doctorate student grant in this context.

We would like to thank the Spanish Institute for Meteorology for their collaboration on the radiosonde ascents and the Institute for Space Studies of Catalonia for their collaborations with the GPS measurements.

The authors wish to thank the CERES Science Team for their support and provision of the data.

Special thanks are also dedicated to Alejandro Bodas Salcedo for his help and suggestions.

The bare soil spectral reflectance used in this work has been reproduced from the ASTER Spectral Library through the courtesy of the Jet Propulsion Laboratory, California Institute of Technology, Pasadena, California.